Journal Pre-proof

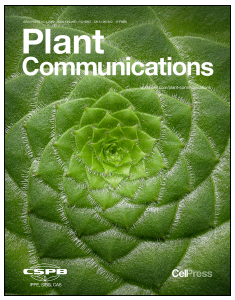


# Bacterial community-emitted volatiles regulate Arabidopsis growth and root architecture in a distinct manner from those from individual strains

Gözde Merve Türksoy, Miroslav Berka, Kathrin Wippel, Anna Koprivova, Réjane Audrey Carron, Lioba Rüger, Martin Černý, Tonni Grube Andersen, Stanislav Kopriva

PII: S2590-3462(25)00113-0

DOI: https://doi.org/10.1016/j.xplc.2025.101351

Reference: XPLC 101351

To appear in: *PLANT COMMUNICATIONS*

Received Date: 24 August 2024

Revised Date: 26 February 2025

Accepted Date: 2 May 2025

Please cite this article as: Türksoy, G.M., Berka, M., Wippel, K., Koprivova, A., Carron, R.A., Rüger, L., Černý, M., Andersen, T.G., Kopriva, S., Bacterial community-emitted volatiles regulate Arabidopsis growth and root architecture in a distinct manner from those from individual strains, *PLANT COMMUNICATIONS* (2025), doi: https://doi.org/10.1016/j.xplc.2025.101351.

# Bacterial community-emitted volatiles regulate Arabidopsis growth and root architecture in a distinct manner from those from individual strains

Gözde Merve Türksoy[1,2], Miroslav Berka[3], Kathrin Wippel[1,4], Anna Koprivova[2], Réjane Audrey Carron[1], Lioba Rüger[1], Martin Černý[3], Tonni Grube Andersen[1**] and Stanislav Kopriva[2**]

1: Max Planck Institute for Plant Breeding Research, Carl-von-Linne-Weg 10, 50829, Cologne, Germany

2: Institute for Plant Sciences, Cluster of Excellence on Plant Sciences (CEPLAS), University of Cologne, 50674 Cologne, Germany; Germany

3: Department of Molecular Biology and Radiobiology, Faculty of AgriSciences, Mendel University in Brno, Brno, Czech Republic

4: Swammerdam Institute for Life Sciences, Faculty of Science, University of Amsterdam, Science Park 904, 1098 XH Amsterdam, The Netherlands

** Corresponding authors: tandersen@mpipz.mpg.de and skopriva@uni-koeln.de

Running title: Bacterial VOCs in community context

Short summary:

This study reveals that the effects of bacterial community-produced volatiles on Arabidopsis growth and root architecture are an emergent property beyond the sum of effects by individual strains. Correlation between composition of the volatile bouquets and growth promotion identified several plant growth promoting volatiles. Further analysis showed that exposure to bacterial volatiles results in dynamic alteration of metabolite profiles of the roots and root exudates, ultimately altering colonization of the roots by the bacteria.

**Abstract**

Volatile organic compounds (VOCs) as infochemicals are important means of communication between bacteria and plants. Bacterial VOCs can promote plant growth and protect plants against biotic or abiotic stresses. To date, most studies have focused on VOCs from single bacterial strains, therefore, very little is known about community-emitted VOCs and their function in modulating plant phenotypes. We showed that VOCs from a root-derived 16 strains synthetic community affect *Arabidopsis* growth and root system architecture, while VOCs from the individual strains trigger a range of different effects. Removing key species from the community affected the relative abundances of other strains and altered VOCs composition, however, the effect on plant growth remained the same. We therefore concluded that bacterial VOCs-induced modulation of plant responses in the rhizosphere may be an emergent property of bacterial communities rather than depending on individual species. Furthermore, altogether we detected 135 different volatiles from individual strains, the most abundant compound emitted by the communities being dimethyl disulfide (DMDS). From correlation analysis we predicted several sulfur-containing compounds to promote plant growth and revealed that exposure to two such VOCs, along with DMDS, leads to plant growth promotion. We also identified plant mutants unable to profit from the DMDS, pointing to an assimilation into S-methylcysteine as a possible mechanism of its action. Finally, we propose that the ecological function of VOCs might be an early signalling alert to prime plants for interaction with the community and through modulation of the exudate composition and accumulation of defense compounds, leading to altered colonization of the plants by the bacteria.

Key words: *Arabidopsis*, bacterial volatiles, synthetic communities, sulfur, dimethyl disulfide, plant-microbe interactions

## Introduction

In nature, roots of healthy plants associate with a diverse set of microorganisms, collectively termed the root microbiota (Bai et al., 2015; Bulgarelli et al., 2013). These microbial communities – in particular bacteria – have been shown to be beneficial for their host, protecting from abiotic and biotic stress and promoting growth through nutrient acquisition and manipulating host phytohormone levels (Castrillo et al., 2017; Harbort et al., 2020; Trapet et al., 2016; Zhang et al., 2019). Additionally, plants can communicate on short distance and shape their microbiome by secreting metabolites belowground, known as root exudates (Basak et al., 2024; Koprivova & Kopriva, 2022; Stringlis et al., 2018). While most attention has been given to communication from the plant to the microbiome, this communication is biidirectional. One important means of the bacterial communication are bacterial volatile organic compounds (VOCs). Due to their nature (low molecular mass, low boiling point and high vapor pressure), VOCs can be transmitted as signals on long and short distance through air, water and soil (Schulz & Dickschat, 2007). Bacterial-emitted VOCs are chemically diverse and can make up complex "bouquets" that consists of different compounds with emergent, overlaying properties that depend on growth substrate and environmental conditions (Blom et al., 2011; Fincheira & Quiroz, 2018). The VOCs are derived from major biosynthesis pathways of primary metabolism, fermentation, sulfur metabolism, fatty acid metabolism, or terpene synthesis (Peñuelas et al., 2014; Schulz & Dickschat, 2007; Weisskopf et al., 2021). Examples of VOCs produced through primary metabolism include compounds derived from valine, leucine, or isoleucine, such as the 2-methylbutanoic acid, 3-methylbutanoic acid, and methylpropanoic acid (Peñuelas et al., 2014). Such VOCs tend to be common components of the VOCs bouquets rather than being specific to a limited number of bacterial strains (Ryu et al., 2020), although for example 1-undecene, produced by the fatty acid pathway (Lo Cantore et al., 2015; Popova et al., 2014) is limited to *Pseudomonas* strains. In contrast, the VOCs produced via secondary metabolism include bacterial family-specific compounds, such as 2,5-diisopropylpyrazine produced from valine by *Paenibacillus polymyxa* and *Chondromyces* (Beck et al., 2003; Blom et al., 2011; Schulz & Dickschat, 2007) and the terpenoid geosmin detected in actinobacteria, myxobacteria and cyanobacteria (Martín-Sánchez et al., 2019). Some VOCs are even strain-specific, such as sodorifen produced through the terpene biosynthesis pathway by *Serratia plymuthica* (Weise et al., 2014) and polyketide streptopyridine from *Streptomyces* (Groenhagen et al., 2014). However, they can also be produced commonly across the bacterial kingdom such as sulfur-containing VOCs dimethyl sulfide, dimethyl disulfide, dimethyl trisulfide, and aromatic compounds indole and 2-phenylethanol (Ryu et al., 2020; Weisskopf et al., 2021).

A large number of bacterial strains have been reported to modulate plant growth, leading to increased biomass and alterations in the root system architecture (Groenhagen et al., 2013; Ryu et al., 2003). One of the best described bacterial models for such plant growth promotion studies is *Pseudomonas simiae* WCS417 (Pieterse et al., 2021). *P. simiae* WCS417 was first isolated from the wheat rhizosphere. It triggers a direct plant growth promotion (PGP) and induces systemic resistance in the host (Pieterse et al., 1996; Pieterse & Van Loon, 1999). WCS417 acts as a biocontrol agent and suppresses wheat disease caused by the soil-borne fungus *Gaeumannomyces graminis* var. t*ritici* (Lamers et al., 1988). Additionally, it protects plants against abiotic stress, e.g., it was shown to increase drought tolerance in peppermint (Chiappero et al., 2019), or salt tolerance in *A. thaliana* (Loo et al., 2022). Moreover, VOCs produced by WCS417 enhance plant growth and induce changes in root architecture, increasing lateral root and root hair density in a manner similar to when the bacteria are cultivated in direct contact with the plant (Blom et al., 2011; Zamioudis et al., 2013). Most VOCs-related studies have been conducted with single bacterial strains, or with low-diversity bacterial communities focusing on community richness effects (Raza et al., 2021) or on their ability to affect plant health through disease suppression in natural environments (Gfeller et al., 2022). Bacterial VOCs in natural ecosystems are also important, e.g. for modulating insect behaviour and attractivity of plant hosts for insects (Zhang et al., 2024). Interestingly, the greatest PGP effects were observed at the lowest community richness, while intermediate richness promoted pathogen suppression by VOCs (Raza et al., 2020) .Similarly, reduced community diversity increased VOC emissions from soil, but reduced the number of individual VOCs (Abis et al., 2020) . However, another study reported that with increased species richness within a bacterial family, both the pathogen suppression and PGP effects were increased (Wang et al., 2021). Thus, the framework for understanding root bacterial VOCs-mediated modulations of plants in a close-to-nature bacterial community context seems still not to be sufficiently developed (Weisskopf et al., 2021). Synthetic communities (SynComs) as representatives of the phylogenetic bacterial diversity in natural soils provide a powerful tool to analyze the mechanisms of plant-microbe interactions and functions of microbiome, including the role of bacterial VOCs (Martins et al., 2023; Vorholt et al., 2017). For example, SynComs representing 16 families of bacteria isolated from Arabidopsis roots have been used to show host preference of commensal bacteria (Wippel et al., 2021).

In this work we focus on how VOCs derived from root microbiome bacterial communities affect growth of *Arabidopsis* and its root architecture. We show that, within a 16-member SynCom, bacteria-bacteria interactions affect the community VOC profiles, resulting in emergent

properties of the VOC bouquets. We identified several VOCs with PGP properties and proposed the mechanism by which DMDS promotes plant growth. We suggest that bacterial VOCs might function as signalling compounds to prime plants for interactions with the bacterial community through modulation of root exudates and accumulation of defense compounds.

## Results

### VOCs from a 16 member SynCom and its individual strains affect *Arabidopsis* growth and root architecture

To study how bacterial VOCs affect *Arabidopsis* seedlings, we chose a previously established and characterised 16-member SynCom (16 SC; (Wippel et al., 2021)). This SynCom consists of strains of 16 families selected from the At-RSPHERE strain library isolated from roots of *Arabidopsis* grown in a natural soil (Bai et al., 2015). It covers a broad taxonomic range of bacteria from families found also in the roots of other plant species (Bai et al., 2015; Wippel et al., 2021); Supplementary Figure 1B). By cultivating plants alone (control), with bacteria mixed in the plant growth medium (direct bacterial contact; DBC), with bacteria in a separate compartment (non-bacterial contact; NBC), and in combination of both DBC and NBC (Supplemental Figure S1A), we assessed to what extent this 16 SC modulates plant growth. In line with previous findings (Durán et al., 2018; Wippel et al., 2021), in the DBC configuration, the 16 SC significantly increased the whole plant fresh weight compared to control (Figure 1A; Supplemental Figure S2). Intriguingly, also in the NBC and the combined configuration, the fresh weight was significantly increased (Figure. 1A). Both NBC and combined treatments led to a significant decrease in primary root length (PRL) and a concurrent increase in lateral root numbers (LRN), which were not affected in the DBC-treated roots (Figure 1B and C). Thus, the VOCs produced by a community of root-associated bacteria induce growth promotion and modulate root architecture.

To disentangle these effects, we determined how individual members of the 16 SC affected *Arabidopsis* plants in the NBC configuration. As a positive control, we employed the *Pseudomonas* strain WCS417, known to trigger growth promotion in *Arabidopsis* seedlings through VOCs (Pieterse et al., 2021; Zamioudis et al., 2015). Interestingly, from the 16 strains included in the 16 SC only R77 had the same effect on all plant traits as the 16 SC, whereas VOCs from 4 strains, R685, R101, R61, and R480, did not significantly affect the plants (Figure 1D, Supplemental Figure S3). Plants exposed to VOCs from WCS417 and 7 SynCom strains

(R83, R131, R77, R29, R935, R265, and R68) showed a significant increase in the total fresh weight, similar to the 16 SC (Figure 1D). Four strains, R131, R77, R935, and R418, showed a similar effect of their VOCs on PRL as the 16 SC, however, R695 and R142 had an opposite effect and triggered an increase in PRL (Figure 1D). Six strains (R83, R123D2, R77, R29, R418, and R1310) promoted LRN similar to 16 SC, whereas WCS417, R935, R68, and R142 showed reduced LRN when compared to controls (Figure 1D). This allowed us to characterize the strains as producing plant growth promoting VOC blends (PGPs) and those with VOC bouquets unable to promote growth (non-PGPs). Taken together, the individual strains elicited a range of distinct responses affecting the shoot biomass and/or root architecture that overall differ from that of the 16 SC. Thus, the plant response may result from dominant key species present in the 16 SC, or it may be an emergent property from species influencing each other in a mixed community.

**GC-MS analysis reveals distinct yet overlapping VOC profiles in communities and individual strains**

Next, to find out which compounds might affect the plant phenotype we conducted Gas Chromatography-Mass Spectrometry (GC-MS) analysis of the VOCs emitted by 16 SC and individual strains. In total 135 different VOCs were detected, including sulfur-containing volatiles, terpenes, various alcohols, or ketones (Supplemental Table S1). In the VOC blend from 16 SC, 55 compounds were identified, while the number of compounds in the individual strains ranged from 5 VOCs in R101 to 62 in R83. Thus, clearly, not all of the compounds emitted by the individual strains were present in the SynCom VOC buquet. The principal component analysis (PCA) of the VOC profiles indicated that all strains had distinct profiles that differed from that of the 16 SC (Figure 2A). The R83 not only produced the most VOCs, it also showed the most distinct VOC profile (Figure 2A), which is likely caused by the several unidentified terpene compounds produced only by this strain (Supplemental Table S1). Fifty seven compounds were found only in VOC blends of a single species, whereas two compounds, the sulfur-containing VOCs dimethyl disulfide (DMDS) and dimethyl trisulfide, were detected in all strains, but in varying abundance (Supplemental Table S1). DMDS is known to confer growth promotion (Meldau et al., 2013; Tyagi et al., 2019), thus it is not surprising that the highest emitters of DMDS were the PGP strains R83, R935 and WCS417, all emitting more DMDS in monoculture than in the 16 SC community (Figure 2B). (Meldau et al., 2013; Tyagi et al., 2019). In contrast, strains producing DMDS concentrations similar to the 16 SC were

both from PGP (R29, R68 and R77) and non-PGP groups (R418, R142, R1310) of strains, while low DMDS emitters were mostly non-PGP strains (R685, R61, R101, R480, R123D2) with the exception of R265 and R131 (Figure 2B). It is thus unlikely that DMDS is solely responsible for the observed *Arabidopsis* growth modulation through 16 SC VOCs.

To determine which strains are driving the VOC profiles of the 16 SC community we analysed the composition of the 16 SC after ten days of growth, using 16S rRNA gene amplicon sequencing. Interestingly, although the community was assembled in equal proportion of the 16 strains, after 10 days it was dominated by R83, R935, and R68 (Figure 2C). These three strains together accounted for about 90% of detected bacterial DNA isolated from the community. Thus, while the VOC profiles from the individual strains are complex with some common and some specific compounds, the community VOC profile might be formed by a few dominating strains.

**VOCs from communities show beneficial effects beyond the combination of individual strains.**

To find out whether the dominant bacterial strains, R935, R83, and R68 are responsible for the effects of 16 SC VOCs on the plants, we performed drop-out experiments, where these strains were omitted from the SynCom individually and in combination. These reduced SynComs were then grown with plants in the NBC configuration. In all drop-out combinations, the fresh weight of exposed plants was significantly higher than the control (Figure 3A). Moreover, we also observed a significant reduction of PR length in all combinations (Figure 3B). It is, thus, likely that the effect of VOCs from the full SynCom on plants is an emergent trait of the bacterial community and not caused by a few dominant strains. We, therefore, asked, whether it may be the less abundant strains to have important roles for the community VOCs and exposed plants to VOCs from the 16 SC missing PGP strains R265 and R131, or non-PGP R123D2 (Figure 1D). As with the previous drop-out communities, these showed the same PGP properties of their VOCs as the 16 SC and the R935-drop-out as a control (Supplemental Figure S4). Thus loss of one or more strains does not significantly alter the impact of 16 SC VOCs on Arabidopsis growth.

Since the drop-out communities had the same effect on the plants as the full 16 SC, we examined whether and how their VOC profiles changed. Overall, there were clear differences in the VOCs composition (Figure 3C; Supplemental Table S2). DMDS was the dominant VOC in most of

the drop-out communities (Figure 3D), with the exception of the ones omitting R935 alone or in combination with R83, however, further exclusion of R68 increased the DMDS abundance again (Figure 3D). Interestingly, loss of the highest DMDS producer R83 did not lower the DMDS concentration in the VOCs compared to full 16 SC. Likewise, terpene and undecene production was lost in the absence of R83 and R68, respectively (Figure 3D).

Since removal of the dominant strains impacted the profiles of major VOCs only moderately, we asked how the loss of these strains affects the composition of these SynComs using 16S rRNA profiling. PCA of the beta-diversity (Bray-Curtis dissimilarities) revealed a very distinct separation of the drop-out communities (Supplementary Figure S5A). Removal of the three dominant strains had a strong impact on community structure but did not appear to disturb the measured VOC-mediated effects on plants. The three dominant strains R935, R68, and R83 continued to dominate the drop-out communities, unless all three were removed (Supplemental Figure S5B). For quantitative analysis, for each drop-out community we adjusted the relative abundance (RA) in 16 SC by *in silico* removing the reads of the omitted strains before the RA calculation. Interestingly, the removal of R68 resulted in increased RA of R83 and, *vice versa*, omission of R83 led to increased RA of R68, whereas leaving out R935 did not affect these two strains (Figure 3E). The removal of the dominant strains, however, impacted also the RAs of the other strains, compared to the full 16 SC (Figure 3E). Thus, for example, removal of R68 and R83 alone or in combination with R935 led to increased RA of R101, a non-PGP strain. Likewise, removal of R935 resulted in increased RA of PGP strain R77. The greatest impact on the RAs of other strains was caused by the removal of all three strains, but the omission of R83 and R68 affected the RAs in a similar way (Figure 3E). Nevertheless, despite these large changes in the bacterial abundances and community composition the emitted VOC blends still influenced the plant in a similar manner as the full SynCom. This indicates that the communities may adjust their composition and/or metabolism to produce a growth-promoting VOC blend and act thus differently than just a sum of its individuals.

To further investigate these emergent properties, we analyzed two additional partial SynComs, composed solely from strains that individually showed either a PGP or non-PGP effect (Figure 1D). VOCs from both the PGP and non-PGP communities triggered a significant growth promotion, not different from the 16 SC (Figure 4A). Similarly, VOCs from both PGP and non-PGP communities led to a significantly shorter PR length but not to the same degree as 16 SC VOCs (Figure 4B). Comparing the community profiles revealed that the removal of nine non-PGP strains did not alter the dominance of strains R83, R935, R68 in the PGP community (Figure 4C). The non-PGP community, composed from nine strains, was dominated by three

strains, R101, R142, and R61. The R101 and R142 showed an increased RA in most of the drop-out communities, indicating that in the 16 SC they might be suppressed by the dominant strains. VOC profiling again showed DMDS emission in both communities at similar levels and comparable to 16 SC, while only the PGP community produced 1-undecene and the terpenes, since the producers of these VOCs, R68 and R83, respectively, were present only there (Figure 4D; Supplemental Table S2). In conclusion, a combination of strains which individually do not promote growth resulted in growth promotion and similar root system changes, supporting the conclusion that communities as a whole have new emerging properties beyond the mere combination of individual strains.

**Characterization of plant growth promoting volatiles from 16 SC community**

To identify further putative PGP volatiles, we correlated the VOC data with the plant fresh weight gains (Figure 5A, Supplemental Table S3). The representation of variable importance for the projection (VIP) values suggested that three compounds, 2-methyl-5-(methylthio)-furan (2M5MTF), 2-methyl-5-(methylthio)-thiophene, and 2,4-dithiapentane (2,4-DTP), may possess a PGP activity on Arabidopsis. We selected the 2M5MTF and 2,4-DTP for verification of their PGP properties, together with three other VOCs, the ubiquitous DMDS, S-methyl thiobutyrate (SMTB), as well as the well characterised anti-fungal or anti-oomycete VOC, 1-undecene (C11:1) (Hunziker et al., 2015; Lo Cantore et al., 2015). To test whether these VOCs might be responsible for the observed plant phenotypes, we applied pure compounds instead of the SynComs in the NBC setup. Indeed, as previously observed (Tyagi et al., 2019), the application of 50 µl of 50 µM DMDS led to significant growth promotion, similar to 16 SC (Figure 5B). The same was true for the 2M5MTF and 2,4-DTP, predicted to have PGP properties (Figure 5A). On the other hand, neither SMTB nor 1-undecene affected the fresh weight of the exposed *Arabidopsis* plants (Figure 5B). Interestingly, when the VOCs were tested in different concentrations, except of 2,4-DTP, all the growth promoting compounds lost this effect at the highest 500 µM concentration, while the SMTB was toxic in high concentration (Supplemental Figure S6). Overall, these results show that different VOCs emitted by the 16 SC might contribute to the 16 SC VOC effects on shoot growth.

Since DMDS is a ubiquitous VOC and the sulfur from DMDS can be assimilated by plants (Meldau et al., 2013), we assessed the mechanisms of its PGP effect. DMDS can produce methanethiol, which in plants is a naturally occurring metabolite, originating from methionine degradation by the methionine γ-lyase (MGL) (Figure 5C) (Rébeillé et al., 2006). Methanethiol

283 can be further degraded to hydrogen sulfide, formaldehyde, and hydrogen peroxide by
284 methanethiol oxidase (MTO), which in animals is represented by selenium binding proteins
285 (SELENBP) (Philipp et al., 2023). Alternatively, it can be incorporated into the precursor of
286 cysteine, O-acetylserine (OAS), to form S-methylcysteine (Rébeillé et al., 2006). To find out
287 which of these reactions are important for DMDS-triggered growth promotion, we assessed the
288 growth promotion of *Arabidopsis* mutants defective in these pathways after exposure to DMDS.
289 The *mgl* and *sbp1* (mutant in homologue of SELENBP) mutants showed increases in growth
290 when exposed to DMDS to a similar extent as the WT Col-0 (Figure 5D), making the MTO an
291 unlikely pathway of DMDS assimilation. On the other hand, two mutants in OAS thiollyase,
292 *oastlA* and *oastlBC*, where the main cytosolic isoform and both plastidic and mitochondrial
293 isoforms are disrupted, respectively (Wirtz & Hell, 2006), lost the ability to profit from DMDS
294 exposure (Figure 5D). Combined, these results suggest that the OAS pathway is essential for
295 this effect. This was further strengthened by the observation of a similar loss of growth
296 promotion in the *serat2;2*, which lacks the mitochondrial isoform of serine acetyltransferase,
297 the enzyme synthesizing the putative acceptor of the methanethiol OAS (Figure 5D). This
298 indicates that DMDS from 16 SC (and other bacteria) is incorporated into the plant organic
299 sulfur pool through reaction with OAS producing S-methylcysteine. The further fate of this
300 compound is, however, unknown. The *oastlA* and *oastlBC* mutants, though, still increased their
301 growth upon exposure to VOCs from the 16 SC (Supplemental Figure S7), bringing another
302 evidence that the PGP effect of the VOCs is multifaceted and conferred by multiple compounds.

303

304 **VOCs act as an early signal to prime plant colonization by bacteria**

305 We then asked what the physiological relevance of the bacterial VOC signalling might be. We
306 hypothesised that the bacterial VOCs may prime the plants for the interaction with the
307 microorganisms and thus VOC-treated plants would assemble different community. Therefore,
308 we first grew plants for 5 days with or without 16 SC VOCs and transferred them into DBC or
309 control conditions for another 7 days. VOC pre-treatments resulted in plant growth promotion
310 irrespective of the presence of 16 SC in the agar (Figure 6A). We then determined the
311 composition of the root-associated microbes using 16S rRNA profiling. Indeed, the pre-
312 treatment with 16 SC VOCs had a significant impact on the composition of the root-associated
313 community. Surprisingly, in the control plants, after 7 days on the plate containing the 16 SC,
314 the root microbiome was completely dominated by R68, which accounted for approximately
315 90% of all reads. However, when the plants were exposed to the VOCs before transfer to 16

316 SC, the root-associated community changed significantly, since the RA of R101, R1310, and
317 R1310 increased (Figure 6B). Thus, it seems that the VOCs indeed prime the plants for
318 colonization with bacteria. Interestingly, pre-exposure to DMDS in the same setup did not result
319 in growth promotion nor affected the root associated community (Supplemental Figure S8).

320 We then hypothesised that the VOCs trigger metabolic changes in the plants, for example, by
321 altering the synthesis of plant defense compounds or the composition of root exudates, and thus
322 facilitate the colonization. Therefore, the levels of the defense compounds glucosinolates and
323 camalexin in the shoots of plants exposed to 16 SC and the model bacterial strain *Pseudomonas*
324 WCS417 in the NBC setup, as well as control plants were determined. While the levels of
325 aliphatic glucosinolates were not affected by the VOCs, the indolic glucosinolates and
326 camalexin levels were indeed reduced (Figure 6C, D, E). To obtain a deeper insight in the plant
327 metabolic alterations upon exposure to VOCs, we performed a GC-MS analysis of *Arabidopsis*
328 exudates, roots, and shoots at two and five days after exposure to the 16 SC volatiles. We
329 quantified altogether 102 metabolites, from which 71 were detected in the exudates, including
330 many sugars, amino acids, organic acids, and several defense related compounds (Figure 7).
331 Exposure to VOCs from the 16 SC community affected metabolite composition of the exudates,
332 but also both roots and shoots, and the changes showed a clear temporal dynamic. In the
333 exudates, the changes were more profound after 5 days, with majority of metabolites being less
334 abundant in the exudates from VOC treated plants than in the controls. However, remarkably,
335 with the exception of the tricarboxylic (TCA) cycle intermediates, such as citrate, oxoglutarate,
336 and malate and the amino acids aspartate and glutamate, the metabolites showed a clear trend
337 of being more highly accumulated in the exudates after two days and less abundant after five
338 days of exposure to VOCs, compared to the respective controls (Figure 7, Supplemental Table
339 S4). After 5 days of VOC treatment, many metabolites were significantly less exuded, in
340 particular the sugars, such as fructose, glucose, and raffinose, sugar related compounds, e.g.,
341 erythritol, galactinol, or glycerate, and the majority of amino acids (Figure 7, Supplemental
342 Table S4). Interestingly, and in agreement with the observed reduction of indolic defense
343 compounds (Figure 6C, E), the pipecolic acid, another metabolite implicated in defense was
344 less abundant in exudates from VOC treated plants than in those from control plants. In addition,
345 the exposure to VOCs resulted in a shift in coumarin profiles manifested by reduced exudation
346 of scopoline and skimmin, and accumulation of esculetin and fraxetin (Figure 7).

347 In general, the VOC effects on root metabolites showed rather opposite trends than in the
348 exudates, in particular the amino acids, which after 2 days were less abundant in roots of VOC
349 treated plants than in controls but accumulated in the exudates, while after five days they were

repressed in the exudates and increased in the roots relative to the non-treated plants. On the other hand, upon VOC exposure, the TCA cycle metabolites were increased also in the roots, particularly citrate and malate, while xylose, raffinose, myo-inositol, ß-alanine, and pantoic acid showed lower abundance than in the controls, like in the exudates. Interestingly, ascorbate and dehydroascorbate were more highly accumulated in roots exposed to the VOCs than in controls, pointing to an increased need for antioxidants in the root. In the shoots, compared to controls, we observed a generally lower accumulation of amino acids, with exception of histidine, asparagine, and glutamine, and also of fructose and sugar phosphates, especially after 5 days VOC treatment. On the other hand, tocopherols and some amino acid derivates accumulated to larger extent (Figure 7). Particularly interesting is the increase of S-methyl cysteine in VOCs exposed roots and shoots, as this compound is the predicted intermediate in DMDS assimilation. Altogether, volatiles from the bacterial community caused a large alteration of metabolite profiles in plant tissues as well as in the root exudates, that seem to facilitate the colonisation of the plant by the bacteria.

## Discussion

### VOCs in 16 SC are not a sum of VOCs from individual strains

One major benefit of using a synthetic community is the ability to compare the composition and effects of its VOCs with those of the individual strains. The strains included in the 16 SC are taxonomically related to strains with demonstrated VOC-mediated effects. For example, the *Pseudomonas* strain R68 and the strains R83 and R29 belonging to Burkholderiales, trigger growth promotion similar to WCS417 and *Burkholderia cepecia*, respectively (Figure 1D) (Pieterse et al., 2021; Zamioudis et al., 2013; Vespermann et al., 2007). Surprisingly, none of the individual strains except R77 affects the plants growth and root architecture in the same way as the 16 SC. Thus, it was unclear if the 16 SC community emits a sum of individual VOCs, whether there is an emerging property due to the interactions among the bacterial strains, or whether the community might be dominated by the most abundant strains.

An efficient way to distinguish between these options is the analysis of drop-out communities (Carlström et al., 2019). We initially selected three strains for the drop-out analysis, R83, R68, and R935, because of their high abundance in the community (Figure 2C) and also because of their unique VOC profiles; R68 as the major producer of 1-undecene and R83 as producer of diverse terpene compounds (Supplemental Table S1). Interestingly, although the composition

of the VOC bouquets of the drop-out communities varied, the effects on the plant, i.e., growth promotion and shortening of primary roots, remained stable (Figure 3A, B). Omission of single low abundant strains, such as R131 or R77, also did not alter the PGP effect of the VOCs, which remained stable even in the PGP community lacking 9 strains compared to 16 SC (Figure 4, Supplemental Figure S4). Thus, despite the community changes in its composition and VOC blends, the VOC effects on the plants remain conserved. It seems, therefore, that the community is able to adapt its VOC production, for example, to compensate the loss of the three major DMDS producers. This agrees with previous studies with plant as well as human microbial communities, where omitting specific strains always resulted in changes in abundance of other community members (Carlström et al., 2019; Wang et al., 2023). However, such changes in abundance are not evenly distributed, e.g., in the human gut microbiome study removal of single strains from 107 members SynCom resulted in a large change in abundance of only eight strains (Wang et al., 2023). Our results are in a full concordance, as we also observed specific effect of the drop-outs on only limited number of remaining strains, however, in our SynCom, abundance of one strain, R77 from the *Caulobacteraceae*, was always increased (Figure 3C). The alterations in the 16 SC were compensatory, so that the function of the drop-out communities, measured as the effect of their VOCs on *Arabidopsis*, did not change compared to full community.

Similarly, the analysis of non-PGP community revealed that the community can indeed acquire a new function that none of the individual strains possesses on its own (Figure 4). This is possible, because collectively we detected 135 different volatiles in the strains forming 16 SC, but only 55 of them were present in the VOCs from this SynCom. While this could be due to different density of the individual strains in pure culture and in the community, it can also emerge as a new property due to microbe-microbe interactions within the community affecting metabolism of the individual strains and their VOCs. Such an emerging function is, for example, the ability of several *Streptomyces* strains to grow on chitin as sole carbon source in a community, but not in a pure culture (McClure et al., 2022). Further acquired community function can be seen, e.g., in the experiments with the maize C7 community, which showed that a full C7 protected the plant against fungal pathogen much better than the individual strains (Niu et al., 2017). The microbe-microbe interactions were clearly detected in the compositions of the drop-out communities (Figure 3E) and are most probably caused by changed balance of bacterial exometabolites, which are a prime determinant of community composition (Getzke et al., 2023). However, also VOCs were shown to affect the composition of the community (Yuan et al., 2017). Such metabolites, including diffusible antimicrobial metabolites, might thus

416 underlie the dominance of the small number of strains in our community (Figure 4C, 6B). In
417 conclusion, the analysis of non-PGP community suggests that the phenotypes caused by the
418 VOCs of the community are distinct from the sum of all its parts and cannot be predicted based
419 on summary of the effects of all individual strains, nor of a few key species.

420

421 **Sulfur containing metabolites and growth promotion**

422 From the 135 compounds detected in the VOC blends, several correlated with the PGP effects
423 of the blends (Figure 5A) and showed a growth promotion as pure chemicals (Figure 5B).
424 Interestingly, all the tested volatiles with PGP effect, 2M5MTF, 2,4-DTP, and DMDS, include
425 sulfur atoms in their structures. Among the 135 VOCs, 24 contain sulfur, and 19 of them are
426 detected among the 16 SC VOCs, forming 34% of the compounds (Supplemental Table S1).
427 However, they are particularly enriched among the most abundant VOCs, where they form 8
428 out of 10 most abundant compounds in 16 SC. Nevertheless, there is no correlation between
429 presence of any individual S-containing VOCs nor number of such VOCs and PGP properties
430 of the VOC buquets, so that the final effect on the plant is conveyed through an interplay of
431 multiple compounds.

432 Among the S-containing compounds, DMDS is of a particular interest as a commonly found
433 volatile compound produced by microbiota and plants, with PGP as well as anti-fungal activities
434 (Lin et al., 2021; Meldau et al., 2013). Also in our experiments, direct exposure of plants to
435 DMDS led to growth promotion (Figure 5). DMDS is synthesized through the sulfur
436 metabolism pathway of a wide range of bacteria, presumably through oxidation of metanethiol,
437 produced from methionine by MGL (Weisskopf et al., 2021). Using radioisotopes, DMDS was
438 shown to be incorporated into plant sulfur-containing compounds and proteins, and to be
439 growth-promoting especially at low sulfur supply (Meldau et al., 2013). DMDS can be used by
440 various bacteria as a sole source of both carbon and sulfur in a pathway with methanethiol,
441 sulfide, formaldehyde and formate as intermediates (Figure 5C) (Smith & Kelly, 1988).
442 However, the mechanism of the assimilation of DMDS in plants is not clear, unlike the
443 assimilation of another sulfur-containing volatile, hydrogen sulfide, which is directly
444 incorporated into cysteine and can even serve as the sole sulfur source for plant growth (Ausma
445 & De Kok, 2019).

446 Our analysis of DMDS assimilation strongly suggests that after reduction of DMDS to
447 methanethiol, it is incorporated into O-acetylserine by OAS-TL to form S-methylcysteine. This

was revealed by the loss of growth promotion by DMDS in the *oastlA* and *oastlBC* mutants as well as in *serat2;2* (Figure 5D) and confirmed by the metabolite analysis which showed a higher accumulation of S-methylcysteine in roots and shoots of plants exposed to VOCs from the 16 SC community emitting DMDS (Figure 7). Correspondingly, OAS-TL transcript was induced by DMDS in tobacco, corroborating the role of OAS-TL in DMDS assimilation (Meldau et al., 2013). The reaction of DMDS with O-acetylserine is well described in plant sulfur metabolism as a part of Met catabolism (Rébeillé et al., 2006) and S-methylcysteine accumulates to significant levels in some plant species, such as common bean and other legumes, onion and garlic (Akash et al., 2014; Chen et al., 1970; Joshi et al., 2019). Production of S-methylcysteine from DMDS increases the availability of reduced sulfur for other metabolic activities, and might, therefore, underlie the effect of DMDS on plant growth. The path of sulfur from S-methylcysteine, however, needs to be further elucidated, but will probably follow the route of Met catabolism. It has to be noted though, that since some high DMDS emitters, such as R695 and R418, did not cause growth promotion, the DMDS cannot be the only growth-promoting substance in the VOC blends. Indeed, while the *oastlA* and *oastlBC* mutants were not able to increase growth after exposure to DMDS, unlike the WT, they gained fresh weight from incubation with the16 SC VOCs (Supplemental Figure S7). This again points to a complex interplay of multiple compounds in modulation of plant response to bacterial VOCs.

**Priming function of bacterial VOCs**

Since in the drop-out experiments the 16 SC community appeared to adapt the emitted VOCs to trigger a consistent alteration of plant growth, there must be a function of the VOCs also for the bacterial community itself. One explanation is that enhanced plant growth increases the availability of organic carbon for the microorganisms and the endophytic space (Weisskopf et al., 2021). However, our experiments revealed additional traits affected by the bacterial VOCs that are beneficial for the microbiota. The reduction in accumulation of defense metabolites, such as camalexin, glucosinolates, pipecolic acid, salicylic acid, scopolin, or skimmin, in the plants and/or root exudates might facilitate the colonization (Figure 6, 7). This could seem to be counterintuitive because camalexin was shown to be necessary for the interaction of plants with beneficial bacteria, i.e., low camalexin was associated with loss of growth promotion (Koprivova et al., 2019). However, it is not clear how camalexin functions and it is possible that the low camalexin actually leads to a greater proliferation of the bacteria and thus stronger biotic stress, preventing the growth gains. Indeed, the loss of indolic phytoalexins, such as

camalexin and indolic glucosinolates, in a *cyp79B2 cyp79B3* Arabidopsis mutant caused the otherwise growth-promoting endophytic fungi *Sebacina vermifera*, *Piriformospora indica*, and *Colletotrichum tofieldiae* to grow extensively in plant tissue and inhibit plant growth up to the level of causing plant death (Hiruma et al., 2016; Lahrmann et al., 2015). In addition, since the colonization of plant root with bacteria triggers an initial defense response including production of reactive oxygene species (ROS) (Teixeira et al., 2021), the accumulation of ascorbate in roots and tocopherol in the shoot might prime the plants and reduce the impact of the ROS. However, the VOCs affect plant metabolism and exudation to a much greater extent than just the defense compounds. The rapid stimulation in exudation of many primary metabolites, sugars and amino acids, increases availability of carbon sources for the bacteria and could promote colonization (Figure 7). On the other hand, the reduced exudation of these metabolites after 5 days can either be caused by increased bacterial growth in the plants or serve as a regulation to limit the attractivity of the rhizosphere for further microorganisms.

Indeed, bacterial VOCs strongly impacted plant metabolism, both primary and secondary, and ultimately, the plants exposed to such VOCs assembled an altered microbial community (Figure 6). This is interesting because traditionally, only plant derived VOCs have been described to act as a factor in microbiome assembly (Liu & Brettell, 2019). For example, a sand sedge *Carex arenaria* changes its volatile profile after infection with a fungal pathogen, which attracts specifically bacteria with anti-fungal properties (Schulz-Bohm et al., 2018). VOCs can also be used to coordinate the assembly of microbiomes in neighbouring plants, as demonstrated in tomato, which after receiving a β-caryophyllene signal alters composition of root exudates, leading to synchronization of the assembled microbiome (Kong et al., 2021). Such signalling can also happen between different plant species, as VOCs from potato and onions affected recruitment of *Pseudomonas* and *Bacillus* strains in tomato rhizosphere, leading to growth promotion (Zhou et al., 2024). Interestingly, the active compound of these VOCs was dipropyl disulfide, another sulfur-containing volatile, similar to DMDS or 2,4-DTP in our study. Also fungi emit VOCs that modulate bacterial metabolism, for example VOCs from the fungal pathogen *Fusarium culmorum* trigger wide ranging transcriptional alterations in *Serratia plymuthica*, leading to synthesis of a volatile terpene compound sodorifen (Schmidt et al., 2017). The effects of bacterial VOCs on other bacteria obtained less attention. It was shown that VOCs from *Bacillus amyloliquefaciens* NJN-6 altered the composition of soil bacterial and fungal communities (Yuan et al., 2017) , however, the effect on plant colonization was not studied. Our findings thus add a different angle to the increasing knowledge on how plants shape their microbiome, because it seems that the assembly might not be controlled only by the

plant but also by the microbes. Whether this mechanism can be exploited to better predict and/or assembly the plant microbial communities remains to be investigated. To better understand the way bacterial communities prime plants to facilitate colonization, the mechanisms of action of individual VOCs alone and in combination need to be investigated both in plants and in the bacterial community, using multi-omics approaches and pathway manipulations. In addition, since our experiments were performed in controlled conditions on agar plates, the transferability of the results in natural soil ecosystems needs to be verified and the effects of VOCs on a longer time scale has to be assessed.

In summary, our work emphasizes that VOCs produced by bacterial communities are likely to be an important factor contributing to plant-microbe communication and shaping bacterial community composition. We show that a bacterial community emits a different VOC buquet than the sum of its members. We reveal that changes in community composition modulate the VOC chemical profiles, but have a minimal effect on the VOCs-mediated plant growth promotion. We identified several compounds in the VOCs from 16 SC community, which cause plant growth promotion and propose a mechanism by which one of the major VOCs, DMDS, exerts its PGP effect. We reveal that the ecological function of the VOCs seems to be the priming of plants for colonization with bacteria, which is achieved by alterations in root exudates and lowering the concentrations of defense metabolites. The ability to manipulate plant performance not only via contact-dependent plant-microbe interactions, but using bacterial VOCs, represents an exciting novel opportunity to improve plant health and may lead to a deeper molecular understanding of the mechanisms that drive overall plant performance in the field.

## Material and Methods

### Plant material and growth conditions

*Arabidopsis thaliana* wild type ecotype Columbia-0 (Col-0) was used for all experiments. For DMDS experiment, mutant lines *oastlA* and *oastlBC* (SP1960, SALK_021183, SALK_000860; Heeg et al., 2008) were obtained from R. Hell, University of Heidelberg, *serat2;2* (Kazusa_KG752), *sbp1* (SALK_058073), and *mgl* (SALK_103805) were obtained from R. Hoefgen, MPI Golm. Seeds were surface-sterilized for 5 min with 70% EtOH, followed by brief wash with 100% EtOH. Dried sterilized seeds were sowed on ½ strength Murashige & Skoog medium (1/2 MS) without sucrose and with 0.8% Bactoagar (pH 5.8) on square plates (Greiner,

120x120 mm). Plates were sealed with Micropore tape, placed in the dark at 4°C for 2-3 days for stratification, then transferred to a growth chamber vertically (16 h light/ 8 h dark cycle, 21/19°C, 100 µmol/m2/s) for germination for 5 days.

**Bacterial growth conditions**

The synthetic community of 16 strains (16 SC) was derived from the SynCom At-SC3 (Wippel et al., 2021), with minor changes (Root1221 was replaced by Root29 and Root1485 replaced by Root418). In addition, the *P. simiae* WCS417 (Pieterse et al., 2021) was used as a positive control. Bacterial strains were cultivated on solid medium containing 15 g/L tryptic soy broth (TSB; Sigma-Aldrich) and 18 g/L Bacto Agar and incubated at 28°C. Information on the individual bacterial strains can be found at At-RSPHERE (http://www.at-sphere.com/) (Bai et al., 2015). Prior to the start of the experiment, liquid cultures were started from single bacterial colonies in 4 mL liquid TSB and incubated shaking overnight at 28°C.

For VOCs profiling of single strains, overnight cultures were diluted to $OD_{600}$=1 in 0.9% sodium chloride and 100 µL of these cultures were inoculated onto 1 mL solid medium containing 15 g/L TSB and 18 g/L Bacto Agar in 10 mL sterile glass headspace vials with crimp caps and incubated at 22°C. To prepare the SynComs, 50 µl each of the 16 bacterial strains ($OD_{600}$ = 1) were combined and vortexed briefly and used for inoculation with the same volume of 100 µL. The bacteria were cultured at 100 µmol $m^{-2}$ $s^{-1}$ photosynthetic photon flux density during a 16 h photoperiod to set the same conditions as during the plate system. The length of cultivation is specified for individual experiments.

**Co-cultivation of plants and bacteria**

For the VOC experiments, warm 1/2 MS medium containing 10 g/L Bacto Agar was poured into square petri dishes (Greiner,120x120 mm), with a small petri dish lid (Greiner, 35x10 mm) positioned at the middle of the bottom part of the plate (Supplementary Figure 1A). The small dish was filled with 4 mL TSB agar medium and allowed to solidify. Five-day-old Col-0 seedlings were placed approximately 1 cm below the top of the square plate system, and for NBC or combined treatments 100 µl of bacterial culture ($OD_{600}$ = 1, in 0.9 % NaCl; individual strains or 16 SC SynCom) were added onto the small petri dish. For controls and DBC experiments, 0.9 % NaCl was added to the small TSB dish. For the DBC conditions, we followed a previously established protocol (Ma et al., 2021). Briefly, strains were adjusted to $OD_{600}$ = 0.2 using 0.9% NaCl, and 150 µl of each bacterial culture were added to 50 ml 40°C warm ½ MS agar medium to yield a final density of $OD_{600}$ = 0.0005, and poured into a square

petri dish. Plates were stored at room temperature overnight before seedling transfer. For control treatment, 150 µl 0.9% NaCl were added into 50 ml 40°C warm ½ MS agar medium. All plates were sealed with Micropore tape after inoculation, and placed vertically in random order in a growth chamber (16 h light/ 8 h dark cycle, 21/19°C, 100 µmol/$m^2$/s). Pictures were taken after 10 days of exposure to VOCs (15 day-old seedlings), where the plants were harvested for fresh weight and metabolites analyses. The primary root length as well as number of lateral roots were quantified from the photographs using manual measurements in Image J (Fiji) (Schindelin et al., 2012).

**Bacterial profiling**

Bacterial DNA for community profiling of pure SynComs was isolated via alkaline lysis. A streak of bacteria was resuspended in 200 µL of 0.9% NaCl, and 12 µL of the sample were added to 20 µL of Buffer I (25 mM NaOH, 0.2 mM EDTA(Na), pH 12), mixed by pipetting, and incubated at 94 °C for 30 min. 20 µL of Buffer II (40 mM Tris-HCl, pH 7.46) was added to neutralize pH. The communities were profiled by amplicon sequencing of the variable v5-v7 regions of the bacterial 16S rRNA gene. Library preparation for Illumina MiSeq sequencing was performed as described previously (Durán et al., 2018). In all experiments, multiplexing of samples was performed by double-indexing (barcoded forward and reverse oligonucleotides for 16S rRNA gene amplification). Amplicon sequencing data was demultiplexed according to their barcode sequence using the QIIME pipeline (Caporaso et al., 2010). Quality-filtered merged paired-end reads were aligned to a reference sequences extracted from the whole-genome assemblies of each individual strain included in a SynCom, using Rbec (v1.0.0) (P. Zhang et al., 2021). A count table was generated, relative abundances calculated, and these were employed for downstream analyses of diversity in R (v4.0.3) with the R package *vegan* (v2.5–6; *vegdist* command with method "bray" for Bray-Curtis dissimilarities). The amplicon data were visualized using the *ggplot2* R package (v3.3.0) (Wickham, 2016). To quantitatively compare the relative abundance of individual strains in the drop-out SynComs vs. the 16-member SynCom, the sequencing reads of the omitted strain were removed from the count table of the full SynCom samples prior to calculation of relative abundances.

For priming experiments, DNA was extracted from plant roots using FastDNA SPIN Kit for Soil (MP Biomedicals, Solon, USA). DNA was eluted with 40 µL nuclease free water. The rRNA amplification, library preparation, amplicon sequencing, and raw data production was performed by Novogene.

**VOC Profiling of Bacterial Strains and Communities**

VOCs were analyzed using a Trace 1300 Gas chromatograph coupled with Q Exactive GC Orbitrap GC-tandem mass spectrometer (Thermo Fisher). One mL of the gas phase was directly injected with TriPlus™ RSH Autosampler (Thermo Fisher, syringe temperature 100 °C) into the injection port (inlet temperature 200 °C, splitless time 0.8 min, purge flow rate 5.0 mL/min, split flow rate 10.0 mL/min) connected to a TG-5SilMS GC column (Thermo Fisher, 30 m × 0.25 mm × 0.25 µm) with He as a carrier gas at a constant flow rate of 1 mL/min.

The SPME fibre assembly divinylbenzene/carboxen/polydimethylsiloxane (DVB/CAR/PDMS, film thickness 50/30 µm, length 1 cm; Supelco) coupled with SPME Fiber Holder (SPME) was used for VOCs collection. VOCs were absorbed into the fibre, exposing it to the headspace in the vial for 35 min at 22 °C. SPME fibre was manually inserted into the injection port for 5 min (inlet temperature 250 °C, splitless time 4 min, purge flow rate 5.0 ml/min, split flow rate 10.0 ml/min) connected to a TG-5SilMS GC column (Thermo Fisher, 30 m × 0.25 mm × 0.25 µm) with He as a carrier gas at a constant flow rate of 1 ml/min. The column was subsequently heated to 320 °C between each sample.

Metabolites were separated over a 23 min gradient (30 °C for 5 min followed by increases of 10 °C/min to 260 °C, and lastly, a 2 min hold time) and ionised using the electron ionisation mode (electron energy 70 eV, emission current 50 µA, transfer line and ion source temperature 250 °C). The mass spectrometer operated in the full scan mode with 60,000 resolutions and a scan range of m/z 30–500, an automatic maximum allowed injection time with automatic gain control set to 1e6 and with internal lock-mass calibration using a background ion $C_5H_{15}O_3Si_3$, (207.0323).

Data were analyzed by Compound Discoverer 3.3 (Thermo Fisher) and searched against NIST2014 and GC-Orbitrap Metabolomics library (peak detection settings: mass tolerance–5 ppm; TIC threshold–10,000; S/N threshold–3, smoothing–9, ion overlap window–90%; group compound settings: RT tolerance–6s). The retention index was calculated using saturated alkane standard solution C8–C40. The metabolites were annotated using spectrum similarity scoring and comparison with the known retention indices. The detectable molecular ion was also taken into account during the identification. Only metabolites that met the identification criteria (score > 75 and $\Delta RI < 2\%$) were included in the final list of identified compounds. Due to the diverse structure of terpenes, only their molecular composition was given without further specification. The identification of DMDS and 1-udecene were confirmed by comparison with the corresponding standard. The final evaluation was done using manual inspection in Skyline

19.1 (Pino et al., 2020). Only peaks fulfilling stringent criteria (absent in blank, at least three specific fragments) were included in the final list of identified compounds.

**Pure Compound Application**

Dimethyl Disulfide (Sigma Aldrich), 2-methyl-5-(methylthio)furan (Thermo Scientific), 2,4-dithiapentane (Sigma Aldrich), and S-methyl thiobutyrate (Thermo Scientific) were diluted to different concentrations (10 µM -500 µM) with EtOH. Cotton bud was placed inside of TSA containing small petri dish in VOC plate system (Supplementary Figure 1A) and 50 µL of the solutions were applied, with 50 µL of EtOH as control. 1-undecene (Sigma Aldrich) was diluted with chloroform (Sigma Aldrich) and 50 µL were applied as above, with 50 µL chloroform as control. After application of pure compounds, the plants were further grown for 10 days sealed with microporse tape as with the bacterial cultures.

**Priming Experiment**

Five day-old plants were transferred into NBC plates (Supplementary Figure 1A), which were either inoculated with 16 SC as described above or with sterile media as control, and grown for 5 days. Both VOCs-treated and non-treated plants were transferred onto DBC plates with 16 SC and cultivated for additional 7 days. As a control, the mock-treated plants were transferred onto plates without any bacteria inoculation. During harvesting, root material was collected under the sterile bench. Root materials were washed with sterile 10 mM $MgSO_4$ and placed into Lyzing matrix E tube and flash frozen in liquid nitrogen. Samples were stored at -80 °C for bacterial DNA extraction as described in community profiling section.

**Analysis of defense compounds**

Camalexin was extracted from ca. 20 mg shoot tissue (fresh weight) in 100 µL of dimethylsulfoxide (DMSO) for 20 min with shaking (1000 rpm). After centrifugation for 20 min at max speed, 20 µL were injected into a Thermo Scientific Dionex UltiMate 3000 HPLC system with Waters Spherisorb ODS-2 column (250 mm x 4.6 mm, 5 µm). The samples were resolved using a gradient of 0.01% (v/v) formic acid (solvent A) and a solvent mixture of 98% (v/v) acetonitrile 2% (v/v) water and 0.01% (v/v) formic acid (solvent B). The gradient program was as follows: 97% A for 5 min; 90% A in 5 min; 40% A in 8 min; 20% A in 2 min; 0% A in 20 min and kept at 0% A for 10 min; 100% A in 2.5 min and kept 100% A for 3.5 min; 97% A in 2 min and kept 97%A for 2 min. Camalexin was detected using a fluorescence detector at an excitation at 318 nm and emission at 368 nm (sensitivity set to 3) exactly as described in (Koprivova et al., 2019).

Glucosinolates were determined in the shoots using the protocol described in Dietzen et al., (2020). Briefly, ca. 25 mg tissue were homogenized in 500 µL hot (70 °C) 70% methanol in water with 2.5 nmol sinigrin as internal standard. The extract was incubated at 70 °C for 45 min, centrifuged and loaded onto columns containing 0.5 ml of DEAE Sephadex A-25. After washing twice with 0.5 mL $H_2O$ and twice with 0.02 M sodium acetate 75 µl sulfatase preparation (30 U) was added to the column and left overnight. The resulting desulfo-glucosinolates were eluted twice with 0.5 ml of sterile $H_2O$, followed by a final elution by 0.25 ml. The combined eluates were resolved by HPLC (Spherisorb ODS2, 250 3 4.6 mm, 5 µm; Waters) using a gradient of acetonitrile in water and detected by UV absorption at 229 nm. The glucosinolates were quantified using the internal standard and response factors as described in Dietzen et al. (2020).

**Exudate analysis**

For exudate collection, the plants transfered for priming in the NBC condition with 16 SC were used. After two or five days of exposure to VOCs the seedlings were transferred into 12 well plates containing 1 ml sterile miliQ water and incubated for 2 h. The one mL exudates in water were collected and flash frozen in liquid nitrogen. Roots and shoots of the plants were separated and frozen for the metabolic analysis.

Exudate samples were spiked with [$^{13}$C]L-valine for internal calibration and were dried in a speed-vacuum concentrator. Samples were derivatized by 10 µl of methoximation solution (40 mg of methoxyamine hydrochloride in 1 ml of pyridine) and incubated for 90 min at 30 °C with continuous shaking. After the incubation, 40 µl of silylation solution (N-methyl-N-trimethylsilyltrifluoroacetamide) was added, and the mixture was incubated for 30 min at 37 °C with continuous shaking, before GC-MS analysis.

**Metabolite analysis and Gas chromatography–mass spectrometry**

Root and shoot samples were lyophilized and homogenized with a grinding ball using a RETSCH mill (5 min, 30 Hz). Homogenized plant samples (six biological replicates per condition) were extracted by incubation with 0.3 ml of pre-cooled (-20 °C) MTBE:MeOH (3:1, v:v) mixture, spiked with [$^{13}$C]L-valine as described in (Berková et al., 2024) with minor modifications. The extracts were vortexed on a RETCH mill (2 min, 30Hz, pre-cooled rack) before being sonicated for 15 min in an ice-cooled sonication bath. Metabolites were further extracted overnight at -20 °C, and the sonication and vortex steps were repeated. The samples were centrifuged for 10 min at 10,000 ×g at 4°C. The supernatant was transferred to new 2-ml

microcentrifuge tubes. The precipitated pellet was washed with 0.15 ml of methanol and vortexed on a RETCH mill (2 min, 30 Hz, pre-cooled rack). The samples were centrifuged for 10 min at 10,000 ×g at 4°C, and the supernatant was combined with the previous supernatant. The samples were mixed and aliquoted into a new 1.5 ml tube and dried in a speed-vacuum concentrator. Samples were dissolved in 15 µl of pyridine and derivatized by 60 µl of silylation solution (N-methyl-N-trimethylsilyltrifluoroacetamide), and the mixture was incubated for 30 min at 37 °C with continuous shaking.

Derivatised metabolites from plant tissue and the exudates were injected onto the TG-5SILMS GC column (Thermo Fisher, 30 m × 0.25 mm × 0.25 µm), separated using a 28 min gradient (70 to 320 °C), and ionized using the electron ionization mode (electron energy 70 eV, emission current 50 µA, transfer line and ion source temperature 250 °C; (Dufková et al., 2023). Data were analyzed by Compound Discoverer 3.3 (Thermo; peak detection settings—5 ppm; TIC threshold—25,000; S/N threshold—3) and searched against NIST2023, the GC-Orbitrap Metabolomics library, and an in-house library. Only metabolites that met the identification criteria (score > 75 and ΔRI < 2%) were included in the final list of identified compounds. The quantitative differences were validated through manual peak assignment in Skyline 19.1 (Pino et al., 2020).

**Statistical analysis**

Pairwise comparisons were performed using a two-tailed Student's t-test in Microsoft Excel (treatment mean vs. control mean). GraphPad version 10 was used to check for normality with Shapiro-Wilk test and to conduct one-way ANOVA with a Tukey's HSD (honestly-significant-difference) post-hoc pairwise T-test when requirements of ANOVA were matched. Alternatively, Kruskal-Wallis or Welch and Brown-Forsythe ANOVA test followed by Dunnett test were performed. Letters and asterisks (*) indicate statistically significant difference of means ($p < 0.05$). Graphs were generated using GraphPad versions 8.02 and 10, R, or Excel. For boxplots, the centre bar depicts the median and the lower and upper box limits depict the 25th and 75th percentile, respectively, whiskers represent minima and maxima, closed dots depict individual samples. PCA analyses were performed in ClustVist (Metsalu & Vilo, 2015). The data are derived from 4 independent petri dishes, each containing 10 plants, and all experiments were repeated at least twice independently.

**Data availability**

All original data and materials will be provided on request to the corresponding authors.

## Funding

TGA is funded by the Max Planck Society (MPG) and the Sofja Kovalevskaja programme of the Alexander von Humboldt foundation. KW is funded through the DFG (German Research Foundation) priority programme SPP2125 DECRyPT – project 466384294. SK and AK research is funded by the DFG under Germany´s Excellence Strategy – EXC 2048/1 – project 390686111 and SPP2125 DECRyPT – project 401836049. GMT thanks for support from the International Max Planck Research School on "Understanding Complex Plant Traits Using Computational and Evolutionary Approaches" and SPP2125 DECRyPT – project 401836049. MB and MČ acknowledge the support of the Czech-German mobility project 8J23DE004. We also thank the German Academic Exchange Service (DAAD) for funding the stay of GMT at the Mendel University in Brno - project 57655738.

## Author contributions

GMT, TGA, RAC, and SK conceptualized the project. GMT, TGA and SK designed the experiments, GMT conducted the experiments, GMT and MB analyzed the data, and TGA and SK supervised the project. KW and LR analyzed bacterial profiling experiments, MB and MČ performed GC-MS and analyzed VOC and metabolite profiles, and AK conducted the analysis of defense compounds. GMT wrote the first draft of manuscript. GMT, KW, MB, MČ, and SK generated figures, SK edited the manuscript, all authors read and approved the manuscript.

## Acknowledgements

We thank Bart Boesten, MPI-PZ, for technical assistance during bacterial profiling and Irene Klinkhammer, University of Cologne, for technical assistance with metabolite analyses. We would like to thank to Corné Pieterse, Utrecht University, for providing the WCS417 strain, Rüdiger Hell, University of Heidelberg, and Rainer Höfgen, MPI Golm, for seeds of the mutants *oastlA*, *oastlBC*, *mgl*, *sbp1*, and *serat2;2*, respectively. We would also like to thank Ka-Wai Ma, MPI-PZ, for the insightful discussions.

## Declaration of interest

The authors declare no competing interests.

## Supplementary data

**Supplemental Figure S1.** Experimental setup.

**Supplemental Figure S2.** Photos of plants after VOC treatments.

**Supplemental Figure S3.** Effects of bacterial VOCs on *Arabidopsis* growth and root system architecture.

**Supplemental Figure S4.** Drop-out SynComs of less abundant strains.

**Supplemental Figure S5.** Diversity of bacterial drop-out SynComs.

**Supplemental Figure S6.** Effects of pure VOCs on plants in concentration gradient.

**Supplemental Figure S7.** Comparison of the effect of 16 SC VOCs and DMDS on mutants in OAST-L.

**Supplemental Figure S8**. Effect of DMDS on community composition.

**Supplemental Table S1.** Results of volatile profiling of the individual bacterial strains and 16 SC using SPME to capture the VOCs and GC-MS.

**Supplemental Table S2.** Results of volatile profiling of the drop-out communities and PGP/Non-PGPs using headspace analysis by GC-MS.

**Supplemental Table S3.** Correlation between the peak areas of individual VOCs and relative plant growth.

**Supplemental Table S4.** Results of metabolite profiling of exudates, roots, and shoots of plants exposed to 16 SC VOCs or not by GC-MS.

## References


Abis, L., Loubet, B., Ciuraru, R., Lafouge, F., Houot, S., Nowak, V., Tripied, J., Dequiedt, S., Maron, P. A., & Sadet-Bourgeteau, S. (2020). Reduced microbial diversity induces larger volatile organic compound emissions from soils. *Scientific Reports*, *10*(1). https://doi.org/10.1038/s41598-020-63091-8

Akash, M. S. H., Rehman, K., & Chen, S. (2014). Spice plant Allium cepa: Dietary supplement for treatment of type 2 diabetes mellitus. *Nutrition*, *30*(10), 1128–1137. https://doi.org/10.1016/J.NUT.2014.02.011

Ausma, T., & De Kok, L. J. (2019). Atmospheric H2S: Impact on plant functioning. In *Frontiers in Plant Science* (Vol. 10). Frontiers Media S.A. https://doi.org/10.3389/fpls.2019.00743

Bai, Y., Müller, D. B., Srinivas, G., Garrido-Oter, R., Potthoff, E., Rott, M., Dombrowski, N., Münch, P. C., Spaepen, S., Remus-Emsermann, M., Hüttel, B., McHardy, A. C., Vorholt, J. A., & Schulze-Lefert, P. (2015). Functional overlap of the Arabidopsis leaf and root microbiota. *Nature*, *528*(7582), 364–369. https://doi.org/10.1038/nature16192

Basak, A. K., Piasecka, A., Hucklenbroich, J., Türksoy, G. M., Guan, R., Zhang, P., Getzke, F., Garrido-Oter, R., Hacquard, S., Strzałka, K., Bednarek, P., Yamada, K., & Nakano, R. T. (2024). ER body-resident myrosinases and tryptophan specialized metabolism modulate root microbiota assembly. *New Phytologist*, *241*(1), 329–342. https://doi.org/10.1111/NPH.19289

Beck, H. C., Hansen, A. M., & Lauritsen, F. R. (2003). Novel pyrazine metabolites found in polymyxin biosynthesis by Paenibacillus polymyxa. *FEMS Microbiology Letters*, *220*(1), 67–73. https://doi.org/10.1016/S0378-1097(03)00054-5

Berková, V., Berka, M., Štěpánková, L., Kováč, J., Auer, S., Menšíková, S., Ďurkovič, J., Kopřiva, S., Ludwig-Müller, J., Brzobohatý, B., & Černý, M. (2024). The fungus Acremonium alternatum enhances salt stress tolerance by regulating host redox homeostasis and phytohormone signaling. *Physiologia Plantarum*, *176*(3). https://doi.org/10.1111/ppl.14328

Blom, D., Fabbri, C., Connor, E. C., Schiestl, F. P., Klauser, D. R., Boller, T., Eberl, L., & Weisskopf, L. (2011). Production of plant growth modulating volatiles is widespread among rhizosphere bacteria and strongly depends on culture conditions. *Environmental Microbiology*, *13*(11), 3047–3058. https://doi.org/10.1111/j.1462-2920.2011.02582.x

Bulgarelli, D., Schlaeppi, K., Spaepen, S., van Themaat, E. V. L., & Schulze-Lefert, P. (2013). Structure and Functions of the BacterBulgarelli, D., Schlaeppi, K., Spaepen, S., van Themaat, E. V. L., & Schulze-Lefert, P. (2013). Structure and Functions of the Bacterial Microbiota of Plants. Annual Review of Plant Biology, 64(1), 807–838. https://doi. *Annual Review of Plant Biology*, *64*(1), 807–838. https://doi.org/10.1146/annurev-arplant-050312-120106

Caporaso, J. G., Kuczynski, J., Stombaugh, J., Bittinger, K., Bushman, F. D., Costello, E. K., Fierer, N., Pẽa, A. G., Goodrich, J. K., Gordon, J. I., Huttley, G. A., Kelley, S. T., Knights, D., Koenig, J. E., Ley, R. E., Lozupone, C. A., McDonald, D., Muegge, B. D., Pirrung, M., … Knight, R. (2010). QIIME allows analysis of high-throughput

community sequencing data. *Nature Methods 2010 7:5*, *7*(5), 335–336. https://doi.org/10.1038/nmeth.f.303

Carlström, C. I., Field, C. M., Bortfeld-Miller, M., Müller, B., Sunagawa, S., & Vorholt, J. A. (2019). Synthetic microbiota reveal priority effects and keystone strains in the Arabidopsis phyllosphere. In *Nature Ecology and Evolution* (Vol. 3, Issue 10, pp. 1445–1454). https://doi.org/10.1038/s41559-019-0994-z

Castrillo, G., Teixeira, P. J. P. L., Paredes, S. H., Law, T. F., De Lorenzo, L., Feltcher, M. E., Finkel, O. M., Breakfield, N. W., Mieczkowski, P., Jones, C. D., Paz-Ares, J., & Dangl, J. L. (2017). Root microbiota drive direct integration of phosphate stress and immunity. *Nature*, *543*(7646), 513–518. https://doi.org/10.1038/NATURE21417

Chen, D. M., Nigam, S. N., & McConnell, W. B. (1970). Biosynthesis of Se-methylselenocysteine and S-methylcysteine in Astragalus bisulcatus. *Canadian Journal of Biochemistry*, *48*(11), 1278–1283. https://doi.org/10.1139/O70-197

Chiappero, J., Cappellari, L. del R., Sosa Alderete, L. G., Palermo, T. B., & Banchio, E. (2019). Plant growth promoting rhizobacteria improve the antioxidant status in Mentha piperita grown under drought stress leading to an enhancement of plant growth and total phenolic content. *Industrial Crops and Products*, *139*, 111553. https://doi.org/10.1016/J.INDCROP.2019.111553

Dietzen, C., Koprivova, A., Whitcomb, S.J., Langen, G., Jobe, T.O., Hoefgen, R., & Kopriva, S. (2020) The Transcription Factor EIL1 Participates in the Regulation of Sulfur-Deficiency Response. *Plant Physiology*, *184,* 2120-2136. https://doi.org/10.1104/pp.20.01192

Dufková, H., Berka, M., Psota, V., Brzobohatý, B., & Černý, M. (2023). Environmental impacts on barley grain composition and longevity. *Journal of Experimental Botany*, *74*(5), 1609–1628. https://doi.org/10.1093/jxb/erac498

Durán, P., Thiergart, T., Garrido-Oter, R., Agler, M., Kemen, E., Schulze-Lefert, P., & Hacquard, S. (2018). Microbial Interkingdom Interactions in Roots Promote Arabidopsis Survival. *Cell*, *175*(4), 973-983.e14. https://doi.org/10.1016/j.cell.2018.10.020

Fincheira, P., & Quiroz, A. (2018). Microbial volatiles as plant growth inducers. *Microbiological Research*, *208*(April 2017), 63–75. https://doi.org/10.1016/j.micres.2018.01.002

Getzke, F., Amine Hassani, M., Crüsemann, M., Malisic, M., Zhang, P., Ishigaki, Y., Böhringer, N., Fernández, A. J., Wang, L., Ordon, J., Ma, K. W., Thiergart, T., Harbort, C. J., Wesseler, H., Miyauchi, S., Garrido-Oter, R., Shirasu, K., Schäberle, T. F., Hacquard, S., & Schulze-Lefert, P. (2023). Cofunctioning of bacterial exometabolites drives root microbiota establishment. *Proceedings of the National Academy of Sciences of the United States of America*, *120*(15). https://doi.org/10.1073/pnas.2221508120

Gfeller, A., Fuchsmann, P., De Vrieze, M., Gindro, K., & Weisskopf, L. (2022). Bacterial Volatiles Known to Inhibit Phytophthora infestans Are Emitted on Potato Leaves by Pseudomonas Strains. *Microorganisms*, *10*(8). https://doi.org/10.3390/microorganisms10081510

877 Groenhagen, U., Baumgartner, R., Bailly, A., Gardiner, A., Eberl, L., Schulz, S., & Weisskopf,
878 L. (2013). Production of Bioactive Volatiles by Different Burkholderia ambifaria Strains.
879 *Journal of Chemical Ecology*, *39*(7), 892–906. https://doi.org/10.1007/S10886-013-
880 0315-Y/FIGURES/6

881 Groenhagen, U., Maczka, M., Dickschat, J. S., & Schulz, S. (2014). Streptopyridines, volatile
882 pyridine alkaloids produced by Streptomyces sp. FORM5. *Beilstein Journal of Organic*
883 *Chemistry*, *10*, 1421–1432. https://doi.org/10.3762/bjoc.10.146

884 Harbort, C. J., Hashimoto, M., Inoue, H., Niu, Y., Guan, R., Rombolà, A. D., Kopriva, S.,
885 Voges, M. J. E. E. E., Sattely, E. S., Garrido-Oter, R., & Schulze-Lefert, P. (2020). Root-
886 Secreted Coumarins and the Microbiota Interact to Improve Iron Nutrition in
887 Arabidopsis. *Cell Host & Microbe*, *28*(6), 825-837.e6.
888 https://doi.org/10.1016/J.CHOM.2020.09.006

889 Heeg, C., Kruse, C., Jost, R., Gutensohn, M., Ruppert, T., Wirtz, M., & Hella, R. (2008).
890 Analysis of the Arabidopsis O-Acetylserine(thiol)lyase Gene Family Demonstrates
891 Compartment-Specific Differences in the Regulation of Cysteine Synthesis. *The Plant*
892 *Cell*, *20*(1), 168–185. https://doi.org/10.1105/TPC.107.056747

893 Hiruma, K., Gerlach, N., Sacristán, S., Nakano, R. T., Hacquard, S., Kracher, B., Neumann,
894 U., Ramírez, D., Bucher, M., O'Connell, R. J., & Schulze-Lefert, P. (2016). Root
895 Endophyte Colletotrichum tofieldiae Confers Plant Fitness Benefits that Are Phosphate
896 Status Dependent. *Cell*, *165*(2), 464–474. https://doi.org/10.1016/J.CELL.2016.02.028

897 Hunziker, L., Bönisch, D., Groenhagen, U., Bailly, A., Schulz, S., & Weisskopf, L. (2015).
898 Pseudomonas Strains Naturally Associated with Potato Plants Produce Volatiles with
899 High Potential for Inhibition of Phytophthora infestans. *Applied and Environmental*
900 *Microbiology*, *81*(3), 821. https://doi.org/10.1128/AEM.02999-14

901 Joshi, J., Saboori-Robat, E., Solouki, M., Mohsenpour, M., & Marsolais, F. (2019).
902 Distribution and possible biosynthetic pathway of non-protein sulfur amino acids in
903 legumes. *Journal of Experimental Botany*, *70*(16), 4115–4121.
904 https://doi.org/10.1093/JXB/ERZ291

905 Kong, H. G., Song, G. C., Sim, H. J., & Ryu, C. M. (2021). Achieving similar root microbiota
906 composition in neighbouring plants through airborne signalling. *The ISME Journal*,
907 *15*(2), 397–408. https://doi.org/10.1038/S41396-020-00759-Z

908 Koprivova, A., & Kopriva, S. (2022). Plant secondary metabolites altering root microbiome
909 composition and function. In *Current Opinion in Plant Biology* (Vol. 67). Elsevier Ltd.
910 https://doi.org/10.1016/j.pbi.2022.102227

911 Koprivova, A., Schuck, S., Jacoby, R. P., Klinkhammer, I., Welter, B., Leson, L., Martyn, A.,
912 Nauen, J., Grabenhorst, N., Mandelkow, J. F., Zuccaro, A., Zeier, J., & Kopriva, S.
913 (2019). Root-specific camalexin biosynthesis controls the plant growth-promoting effects
914 of multiple bacterial strains. In *Proceedings of the National Academy of Sciences of the*
915 *United States of America* (Vol. 116, Issue 31, pp. 15735–15744).
916 https://doi.org/10.1073/pnas.1818604116

917 Lahrmann, U., Strehmel, N., Langen, G., Frerigmann, H., Leson, L., Ding, Y., Scheel, D.,
918 Herklotz, S., Hilbert, M., & Zuccaro, A. (2015). Mutualistic root endophytism is not

associated with the reduction of saprotrophic traits and requires a noncompromised plant innate immunity. *New Phytologist*, *207*(3), 841–857. https://doi.org/10.1111/NPH.13411

Lamers JG, Schippers B, Geels FP (1988) Soil-borne diseases of wheat in the Netherlands and results of seed bacterization with pseudomonads against Gaeumannomyces graminis var. tritici, associated with disease resistance. In: Jorna ML, Slootmaker LAJ (eds) Cereal breeding related to integrated cereal production. Pudoc, Wageningen. Pp 134-139

Lin, Y. T., Lee, C. C., Leu, W. M., Wu, J. J., Huang, Y. C., & Meng, M. (2021). Fungicidal Activity of Volatile Organic Compounds Emitted by Burkholderia gladioli Strain BBB-01. *Molecules*, *26*(3). https://doi.org/10.3390/MOLECULES26030745

Liu, H., & Brettell, L. E. (2019). Plant Defense by VOC-Induced Microbial Priming. *Trends in Plant Science*, *24*(3), 187–189. https://doi.org/10.1016/J.TPLANTS.2019.01.008

Lo Cantore, P., Giorgio, A., & Iacobellis, N. S. (2015). Bioactivity of volatile organic compounds produced by Pseudomonas tolaasii. *Frontiers in Microbiology*, *6*(OCT), 156562. https://doi.org/10.3389/FMICB.2015.01082/BIBTEX

Loo, E. P. I., Tajima, Y., Yamada, K., Kido, S., Hirase, T., Ariga, H., Fujiwara, T., Tanaka, K., Taji, T., Somssich, I. E., Parker, J. E., & Saijo, Y. (2022). Recognition of Microbe- and Damage-Associated Molecular Patterns by Leucine-Rich Repeat Pattern Recognition Receptor Kinases Confers Salt Tolerance in Plants. *Molecular Plant-Microbe Interactions*, *35*(7), 554–566. https://doi.org/10.1094/MPMI-07-21-0185-FI/ASSET/IMAGES/LARGE/MPMI-07-21-0185-FIF7.JPEG

Ma, K. W., Niu, Y., Jia, Y., Ordon, J., Copeland, C., Emonet, A., Geldner, N., Guan, R., Stolze, S. C., Nakagami, H., Garrido-Oter, R., & Schulze-Lefert, P. (2021). Coordination of microbe–host homeostasis by crosstalk with plant innate immunity. *Nature Plants 2021 7:6*, *7*(6), 814–825. https://doi.org/10.1038/s41477-021-00920-2

Martins, S. J., Pasche, J., Silva, H. A. O., Selten, G., Savastano, N., Abreu, L. M., Bais, H. P., Garrett, K. A., Kraisitudomsook, N., Pieterse, C. M. J., & Cernava, T. (2023). The Use of Synthetic Microbial Communities to Improve Plant Health. *Phytopathology*, *113*(8), 1369–1379. https://doi.org/10.1094/PHYTO-01-23-0016-IA/ASSET/IMAGES/LARGE/PHYTO-01-23-0016-IAF3.JPEG

Martín-Sánchez, L., Singh, K. S., Avalos, M., Van Wezel, G. P., Dickschat, J. S., & Garbeva, P. (2019). Phylogenomic analyses and distribution of terpene synthases among Streptomyces. *Beilstein Journal of Organic Chemistry*, *15*, 1181. https://doi.org/10.3762/BJOC.15.115

McClure, R., Farris, Y., Danczak, R., Nelson, W., Song, H.-S., Kessell, A., Lee, J.-Y., Couvillion, S., Henry, C., Jansson, J. K., & Hofmockel, K. S. (2022). Interaction Networks Are Driven by Community-Responsive Phenotypes in a Chitin-Degrading Consortium of Soil Microbes. *MSystems*, *7*(5). https://doi.org/10.1128/MSYSTEMS.00372-22

Meldau, D. G., Meldau, S., Hoang, L. H., Underberg, S., Wünsche, H., & Baldwin, I. T. (2013). Dimethyl disulfide produced by the naturally associated bacterium bacillus sp B55 promotes Nicotiana attenuata growth by enhancing sulfur nutrition. *The Plant Cell*, *25*(7), 2731–2747. https://doi.org/10.1105/TPC.113.114744

961 Metsalu, T., & Vilo, J. (2015). ClustVis: A web tool for visualizing clustering of multivariate
962 data using Principal Component Analysis and heatmap. *Nucleic Acids Research*, *43*(W1),
963 W566–W570. https://doi.org/10.1093/nar/gkv468

964 Niu, B., Paulson, J. N., Zheng, X., & Kolter, R. (2017). Simplified and representative
965 bacterial community of maize roots. *Proceedings of the National Academy of Sciences of*
966 *the United States of America*, *114*(12), E2450–E2459.
967 https://doi.org/10.1073/PNAS.1616148114

968 Peñuelas, J., Asensio, D., Tholl, D., Wenke, K., Rosenkranz, M., Piechulla, B., & Schnitzler,
969 J. P. (2014). Biogenic volatile emissions from the soil. *Plant, Cell & Environment*, *37*(8),
970 1866–1891. https://doi.org/10.1111/PCE.12340

971 Philipp, T. M., Scheller, A. S., Krafczyk, N., Klotz, L. O., & Steinbrenner, H. (2023).
972 Methanethiol: A Scent Mark of Dysregulated Sulfur Metabolism in Cancer. *Antioxidants*,
973 *12*(9). https://doi.org/10.3390/ANTIOX12091780

974 Piechulla, B., Lemfack, M. C., & Kai, M. (2017). Effects of discrete bioactive microbial
975 volatiles on plants and fungi. *Plant, Cell & Environment*, *40*(10), 2042–2067.
976 https://doi.org/10.1111/PCE.13011

977 Pieterse, C. M. J., Berendsen, R. L., de Jonge, R., Stringlis, I. A., Van Dijken, A. J. H., Van
978 Pelt, J. A., Van Wees, S. C. M., Yu, K., Zamioudis, C., & Bakker, P. A. H. M. (2021).
979 Pseudomonas simiae WCS417: star track of a model beneficial rhizobacterium. In *Plant*
980 *and Soil* (Vol. 461, Issues 1–2, pp. 245–263). Springer Science and Business Media
981 Deutschland GmbH. https://doi.org/10.1007/s11104-020-04786-9

982 Pieterse, C. M. J., van Wees, S. C. M., Hoffland, E., van Pelt, J. A., & van Loon, L. C. (1996).
983 Systemic Resistance in Arabidopsis Induced by Biocontrol Bacteria Is Independent of
984 Salicylic Acid Accumulation and Pathogenesis-Related Gene Expression. *The Plant Cell*,
985 *8*(8), 1225. https://doi.org/10.2307/3870297

986 Pino, L. K., Searle, B. C., Bollinger, J. G., Nunn, B., MacLean, B., & MacCoss, M. J. (2020).
987 The Skyline ecosystem: Informatics for quantitative mass spectrometry proteomics. In
988 *Mass Spectrometry Reviews* (Vol. 39, Issue 3, pp. 229–244). John Wiley and Sons Inc.
989 https://doi.org/10.1002/mas.21540

990 Popova, A. A., Koksharova, O. A., Lipasova, V. A., Zaitseva, J. V., Katkova-Zhukotskaya, O.
991 A., Eremina, S. I., Mironov, A. S., Chernin, L. S., & Khmel, I. A. (2014). Inhibitory and
992 Toxic Effects of Volatiles Emitted by Strains of Pseudomonas and Serratia on Growth
993 and Survival of Selected Microorganisms, Caenorhabditis elegans, and Drosophila
994 melanogaster. *BioMed Research International*, *2014*.
995 https://doi.org/10.1155/2014/125704

996 Raza, W., Wang, J., Jousset, A., Friman, V. P., Mei, X., Wang, S., Wei, Z., & Shen, Q. (2020).
997 Bacterial community richness shifts the balance between volatile organic compound-
998 mediated microbe–pathogen and microbe–plant interactions. *Proceedings of the Royal*
999 *Society B: Biological Sciences*, *287*(1925). https://doi.org/10.1098/rspb.2020.0403

1000 Raza, W., Wei, Z., Jousset, A., Shen, Q., & Friman, V.-P. (2021). Extended Plant
1001 Metarhizobiome: Understanding Volatile Organic Compound Signaling in Plant-Microbe

Metapopulation Networks. *MSystems*, *6*(4). https://doi.org/10.1128/MSYSTEMS.00849-21/SUPPL_FILE/REVIEWER-COMMENTS.PDF

Rébeillé, F., Jabrin, S., Bligny, R., Loizeau, K., Gambonnet, B., Van Wilder, V., Douce, R., & Ravanel, S. (2006). Methionine catabolism in Arabidopsis cells is initiated by a γ-cleavage process and leads to S-methylcysteine and isoleucine syntheses. *Proceedings of the National Academy of Sciences of the United States of America*, *103*(42), 15687–15692. https://doi.org/10.1073/PNAS.0606195103/ASSET/B5D48558-78FA-45F6-A53C-5F369634CD62/ASSETS/GRAPHIC/ZPQ0410637480006.JPEG

Ryu, C. M., Faragt, M. A., Hu, C. H., Reddy, M. S., Wei, H. X., Paré, P. W., & Kloepper, J. W. (2003). Bacterial volatiles promote growth in Arabidopsis. *Proceedings of the National Academy of Sciences of the United States of America*, *100*(8), 4927–4932. https://doi.org/10.1073/pnas.0730845100

Ryu, C.-M., Weisskopf L, & Piechulla B. (2020). Bacterial volatile compounds as mediators of airborne interactions. Singapore: Springer Singapore. https://doi.org/10.1007/978-981-15-7293-7

Schindelin, J., Arganda-Carreras, I., Frise, E., Kaynig, V., Longair, M., Pietzsch, T., Preibisch, S., Rueden, C., Saalfeld, S., Schmid, B., Tinevez, J. Y., White, D. J., Hartenstein, V., Eliceiri, K., Tomancak, P., & Cardona, A. (2012). Fiji: an open-source platform for biological-image analysis. *Nature Methods 2012 9:7*, *9*(7), 676–682. https://doi.org/10.1038/nmeth.2019

Schmidt, R., De Jager, V., Zühlke, D., Wolff, C., Bernhardt, J., Cankar, K., Beekwilder, J., Van Ijcken, W., Sleutels, F., De Boer, W., Riedel, K., & Garbeva, P. (2017). Fungal volatile compounds induce production of the secondary metabolite Sodorifen in Serratia plymuthica PRI-2C. *Scientific Reports*, *7*(1). https://doi.org/10.1038/s41598-017-00893-3

Schulz, S., & Dickschat, J. S. (2007). Bacterial volatiles: the smell of small organisms. *Natural Product Reports*, *24*(4), 814–842. https://doi.org/10.1039/B507392H

Schulz-Bohm, K., Gerards, S., Hundscheid, M., Melenhorst, J., De Boer, W., & Garbeva, P. (2018). Calling from distance: attraction of soil bacteria by plant root volatiles. *The ISME Journal 2018 12:5*, *12*(5), 1252–1262. https://doi.org/10.1038/s41396-017-0035-3

Smith, N. A., & Kelly, D. P. (1988). Isolation and Physiological Characterization of Autotrophic Sulphur Bacteria Oxidizing Dimethyl Disulphide as Sole Source of Energy. *Microbiology*, *134*(6), 1407–1417. https://doi.org/10.1099/00221287-134-6-1407

Stringlis, I. A., Yu, K., Feussner, K., De Jonge, R., Van Bentum, S., Van Verk, M. C., Berendsen, R. L., Bakker, P. A. H. M., Feussner, I., & Pieterse, C. M. J. (2018). MYB72-dependent coumarin exudation shapes root microbiome assembly to promote plant health. *Proceedings of the National Academy of Sciences of the United States of America*, *115*(22), E5213–E5222. https://doi.org/10.1073/PNAS.1722335115/SUPPL_FILE/PNAS.1722335115.SD06.XLSX

Teixeira, P. J. P. L., Colaianni, N. R., Law, T. F., Conway, J. M., Gilbert, S., Li, H., Salas-González, I., Panda, D., Risco, N. M. Del, Finkel, O. M., Castrillo, G., Mieczkowski, P.,

Jones, C. D., & Dangl, J. L. (2021). *Specific modulation of the root immune system by a community of commensal bacteria PLANT BIOLOGY*. *118*, 2100678118. https://doi.org/10.1073/pnas.2100678118/-/DCSupplemental

Trapet, P., Avoscan, L., Klinguer, A., Pateyron, S., Citerne, S., Chervin, C., Mazurier, S., Lemanceau, P., Wendehenne, D., & Besson-Bard, A. (2016). The Pseudomonas fluorescens Siderophore Pyoverdine Weakens Arabidopsis thaliana Defense in Favor of Growth in Iron-Deficient Conditions. *Plant Physiology*, *171*(1), 675–693. https://doi.org/10.1104/pp.15.01537

Tyagi, S., Kim, K., Cho, M., Kui, ·, & Lee, J. (2019). Volatile dimethyl disulfide affects root system architecture of Arabidopsis via modulation of canonical auxin signaling pathways. *Environmental Sustainability 2019 2:2*, *2*(2), 211–216. https://doi.org/10.1007/S42398-019-00060-6

Vespermann, A., Kai, M., & Piechulla, B. (2007). Rhizobacterial volatiles affect the growth of fungi and Arabidopsis thaliana. *Applied and Environmental Microbiology*, *73*(17), 5639–5641. https://doi.org/10.1128/AEM.01078-07

Vorholt, J. A., Vogel, C., Carlström, C. I., & Müller, D. B. (2017). Establishing Causality: Opportunities of Synthetic Communities for Plant Microbiome Research. *Cell Host & Microbe*, *22*(2), 142–155. https://doi.org/10.1016/J.CHOM.2017.07.004

Wang, J., Mei, X., Wei, Z., Raza, W., & Shen, Q. (2021). Effect of bacterial intra-species community interactions on the production and activity of volatile organic compounds. *Soil Ecology Letters*, *3*(1), 32–41. https://doi.org/10.1007/s42832-020-0054-2

Wang, M., Osborn, L. J., Jain, S., Meng, X., Weakley, A., Yan, J., Massey, W. J., Varadharajan, V., Horak, A., Banerjee, R., Allende, D. S., Chan, E. R., Hajjar, A. M., Wang, Z., Dimas, A., Zhao, A., Nagashima, K., Cheng, A. G., Higginbottom, S., … Fischbach, M. A. (2023). Strain dropouts reveal interactions that govern the metabolic output of the gut microbiome. *Cell*, *186*(13), 2839. https://doi.org/10.1016/J.CELL.2023.05.037

Watanabe, M., Kusano, M., Oikawa, A., Fukushima, A., Noji, M., & Saito, K. (2008). Physiological Roles of the β-Substituted Alanine Synthase Gene Family in Arabidopsis. *Plant Physiology*, *146*(1), 310. https://doi.org/10.1104/PP.107.106831

Weise, T., Thürmer, A., Brady, S., Kai, M., Daniel, R., Gottschalk, G., & Piechulla, B. (2014). VOC emission of various Serratia species and isolates and genome analysis of Serratia plymuthica 4Rx13. In *FEMS Microbiology Letters* (Vol. 352, Issue 1, pp. 45–53). https://doi.org/10.1111/1574-6968.12359

Weisskopf, L., Schulz, S., & Garbeva, P. (2021). Microbial volatile organic compounds in intra-kingdom and inter-kingdom interactions. *Nature Reviews Microbiology*, *19*(6), 391–404. https://doi.org/10.1038/s41579-020-00508-1

Wickham, H. (2016). *ggplot2: Elegant Graphics for Data Analysis* (ISBN 978-3-319-24277-4). Springer-Verlag New York.

Wippel, K., Tao, K., Niu, Y., Zgadzaj, R., Kiel, N., Guan, R., Dahms, E., Zhang, P., Jensen, D. B., Logemann, E., Radutoiu, S., Schulze-Lefert, P., & Garrido-Oter, R. (2021). Host preference and invasiveness of commensal bacteria in the Lotus and Arabidopsis root

microbiota. *Nature Microbiology*, *6*(9), 1150–1162. https://doi.org/10.1038/s41564-021-00941-9

Wirtz, M., & Hell, R. (2006). Functional analysis of the cysteine synthase protein complex from plants: Structural, biochemical and regulatory properties. *Journal of Plant Physiology*, *163*(3), 273–286. https://doi.org/10.1016/J.JPLPH.2005.11.013

Yuan, J., Zhao, M., Li, R., Huang, Q., Raza, W., Rensing, C., & Shen, Q. (2017). Microbial volatile compounds alter the soil microbial community. *Environmental Science and Pollution Research*, *24*(28), 22485–22493. https://doi.org/10.1007/s11356-017-9839-y

Zamioudis, C., Korteland, J., Van Pelt, J. A., van Hamersveld, M., Dombrowski, N., Bai, Y., Hanson, J., Van Verk, M. C., Ling, H.-Q. Q., Schulze-Lefert, P., & Pieterse, C. M. J. (2015). Rhizobacterial volatiles and photosynthesis-related signals coordinate MYB72 expression in Arabidopsis roots during onset of induced systemic resistance and iron-deficiency responses. *Plant Journal*, *84*(2), 309–322. https://doi.org/10.1111/tpj.12995

Zamioudis, C., Mastranesti, P., Dhonukshe, P., Blilou, I., & Pieterse, C. M. J. (2013). Unraveling Root Developmental Programs Initiated by Beneficial Pseudomonas spp. Bacteria. *Plant Physiology*, *162*(1), 304–318. https://doi.org/10.1104/PP.112.212597

Zhang, H., Zhu, Y., Wang, Y., Jiang, L., Shi, X., & Cheng, G. (2024). Microbial interactions shaping host attractiveness: insights into dynamic behavioral relationships. In *Current Opinion in Insect Science* (Vol. 66). Elsevier Inc. https://doi.org/10.1016/j.cois.2024.101275

Zhang, J., Liu, Y. X., Zhang, N., Hu, B., Jin, T., Xu, H., Qin, Y., Yan, P., Zhang, X., Guo, X., Hui, J., Cao, S., Wang, X., Wang, C., Wang, H., Qu, B., Fan, G., Yuan, L., Garrido-Oter, R., … Bai, Y. (2019). NRT1.1B is associated with root microbiota composition and nitrogen use in field-grown rice. *Nature Biotechnology*, *37*(6), 676–684. https://doi.org/10.1038/S41587-019-0104-4

Zhang, P., Spaepen, S., Bai, Y., Hacquard, S., & Garrido-Oter, R. (2021). Rbec: a tool for analysis of amplicon sequencing data from synthetic microbial communities. *ISME Communications*, *1*(1). https://doi.org/10.1038/s43705-021-00077-1

Zhou, X., Zhang, J., Shi, J., Khashi U Rahman, M., Liu, H., Wei, Z., Wu, F., & Dini-Andreote, F. (2024). Volatile-mediated interspecific plant interaction promotes root colonization by beneficial bacteria via induced shifts in root exudation. *Microbiome*, *12*(1), 207. https://doi.org/10.1186/s40168-024-01914-w

## Figure legends

**Figure 1**. **Effects of bacterial VOCs on *Arabidopsis* growth and root system architecture**. **A-C** Five day-old *Arabidopsis thaliana* seedlings were transferred onto MS-agar Petri dishes and grown for 10 days without bacteria as a control (ctrl) in a shared headspace with 16 SC SynCom (NBC), with a 16 SC in the agar in a direct bacterial contact (DBC) or a combination of both (Combined) (cf. Supplemental Figure S1). **A)** Fresh weight of whole seedlings compared to control (ctrl = 100%), mean of 3 pooled samples of at least 10 seedlings. **B)** Primary root length compared to control (ctrl = 100%), mean of 30 plants. **C)** Lateral root number compared to control (ctrl = 100%) mean of 30 plants. A-C, Data are shown as boxplots, the centre bar depicts the median, the lower and upper box limits depict the 25th and 75th percentile, respectively, whiskers represent minima and maxima, and dots depict individual samples. Different letters indicate statistically significant differences (one-way ANOVA and Tukey's HSD Test (A); Welch and Brown-Forsythe ANOVA test and Dunnett test (B); Kruskal-Wallis and Dunnett test (C); $p<0.05$ ). **D)** Heat map of the effects of 16 SC, the individual strains forming 16 SC, and *Pseudomonas simiae* WCS417 on *Arabidopsis* fresh weight (FW), primary root length (PRL), and lateral root number (LRN) after 10 days of growth with the VOCs in NBC setup. Results are shown relative to control without bacteria, in percentage calculated from means of three biological replicates containing 10 seedlings each. Asterisks indicate statistically significant differences compared to control via Student t-test ($p<0.05$). For absolute data see Supplemental Figure S3.

**Figure 2. VOC Profiles of Individual Strains. A)** 16 SC, 16 individual strains, and the control *Pseudomonas* WCS417 were grown on TSB media for 2 days, the VOCs were captured with SPME, and analyzed by GC-MS**.** The PCA based on all 135 identified volatiles in 3 biological replicates was performed in ClustVis. Differently colored circles and squares represent plant growth promoting (PGPs) and nonPGP strains, respectively. **B)** Relative abundance of dimethyldisulfide (DMDS) produced by individual strains and 16 SC, determined by SPME capture and GC-MS, and based on peak area, in 3 biological replicates. Shown are means and standard deviations of the peak areas normalised to 16 SC, which was set to 1. Red color indicates strains with a plant growth promoting VOCs blend. **C)** Relative abundance of individual strains in 16 SC using 16S rRNA gene profiling, from 6 biological replicates. Data are shown as boxplots, the centre bar depicts the median, the lower and upper box limits depict the 25th and 75th percentile, respectively, and dots depict individual samples.

**Figure 3. Characterization of Drop-Out Communities.** *Arabidopsis* plants were grown for 10 days in NBC setup in a shared headspace with 16 SC, drop-out communities, where the highly abundant strains were omitted individually or in combination, or without bacteria (ctrl). Shoot fresh weight **(A)** and primary root length **(B)** were determined in 4 replicate plates each containing 10 plants. The results are calculated as percentage relative to control and shown as boxplots with individual values depicted by red dots. Asterisks indicate statistically significant differences to control (Kruskal-Wallis and Dunnett test, $p<0.05$, $n=40$). **C)** PCA of seven VOCs identified with high confidence through headspace GC-MS analysis of VOCs produced by the drop-out communities. Measurements took place after 1 day of growth on TSB media in four biological replicates. **D)** Relative abundance of the 7 VOCs in 16 SC and drop-out communities identified by GC-MS of headspace after 1 day of growth on TSB, based on peak areas in four biological replicates. **E)** The dot plot shows the relative abundance (RA) of each strain in the drop-out community compared to the full 16 SC, obtained by rRNA profiling with 9 biological replicates. The dot size corresponds to the log2 mean RA. The color indicates the log2 fold change of the RA relative to the RA of 16 SC after *in silico* depletion of the relevant strain(s) (see Material and Methods). A circled dot indicates a significant change (Wilcoxon rank sum test, $p<0.05$).

**Figure 4. Analysis of PGPs and Non-PGPs communities.** *Arabidopsis* plants were grown for 10 days in NBC setup in a shared headspace with 16 SC and communities formed from all PGP strains from 16 SC (PGPs) or non-PGP strains (Non-PGPs). Shoot fresh weight **(A)** and primary root length **(B)** were determined in 4 replicate plates each containing 10 plants. The results are calculated as percentage relative to control and shown as boxplots with individual values depicted by red dots. Different letters indicate statistically significant values (one-way ANOVA and Tukey's HSD Test, $p<0.05$, $n=40$). **C)** Relative abundance of the bacterial strains in the individual communities determined by 16S rRNA gene profiling. **D)** Relative abundance of the 7 VOCs in 16 SC, PGPs and Non-PGPs communities identified by GC-MS of headspace after 1 day of growth on TSB, based on peak areas in four biological replicates.

**Figure 5**. **Effects of pure VOCs on plants**. **A)** Candidate VOCs associated with growth responses in Arabidopsis plants. The variable importance in the projection (VIP) plot was derived from orthogonal partial least squares (OPLS) analysis, using growth response as the predictor. VIP is plotted against the Pearson correlation coefficients (p(corr)) from correlations of plant fresh weight and peak area of the individual VOCs. VOCs with abundance significantly correlating with growth are labelled. **B)** *Arabidopsis* plants were grown for 10 days in a shared headspace with 16 SC, or 50 µl of the following VOCs: 50 µM DMDS, 10 µM 2-methyl-5-

(methylthio)-furan (2M5MTF), 50 µM 2,4-dithiapentane (2,4-DTP), 10 µM S-methyl thiobutyrate (SMTB), or 50 µM 1-undecene (C11:1) and shoot fresh weight were determined in 40 plants. The results are calculated as percentage relative to control and shown as boxplots with individual values depicted by dots. Asterisks indicate statistically significant differences to control (Student T-test, $p<0.05$, $n=40$). ns, not significant. **C)** Scheme of possible reactions in assimilation of DMDS. **D)** Wild type Col-0 and mutants *mgl, sbp1, oastlA, oastlBC*, and *serat2;2* were grown for 10 days in a shared headspace with 50 µl of 50 µM DMDS and shoot fresh weight was determined in 40 plants. The results are calculated as percentage relative to control and shown as boxplots with individual values depicted by dots. Asterisks indicate statistically significant differences to control (Student T-test, $p<0.05$, $n=40$). ns, not significant.

**Figure 6. Priming by VOCs**. *Arabidopsis* plants were grown for 5 days on MS-agar plates with or without sharing headspace with the 16 SC community. Afterwards the plants were transferred to plates with or without direct contact with 16 SC and grown for additional 7 days. **A)** FW of the primed (VOC-DBC, VOC-ctrl), non-primed (ctrl-DBC) and control plants (ctrl-ctrl) was determined, calculated as percentage relative to control and shown as boxplots with individual values depicted by dots. Different letters indicate statistically significant differences (Welch and Brown-Forsythe ANOVA test and Dunnett test, $p<0.05$, $n=10$). **B)** The community composition in the roots was analyzed by 16S rRNA gene profiling. The chart shows relative abundance (RA) of the bacterial strains in the individual communities in the roots primed or not by the 16 SC VOCs. **C-E)** *Arabidopsis* plants were grown for 10 days in a shared headspace with 16 SC and *Pseudomonas* WCS417, or without any bacteria (control). The content of camalexin **(C)**, aliphatic glucosinolates **(D)**, and indolic glucosinolates **(E)** were determined by HPLC in eight independent pools of 3 shoots. The results are shown as boxplots with individual values depicted by dots. Different letters indicate statistically significant differences (one-way ANOVA and Tukey's HSD Test, $p<0.05$, $n=8$). ns, not significant.

**Figure 7. Metabolite analysis of the response of Arabidopsis to 16 SC VOCs.** *Arabidopsis* plants were grown for 5 days on MS-agar plates and transferred to new plates with or without sharing headspace with the 16 SC community. After 2 and 5 days exudates, roots and shoots were collected from the treated plants, and subjected to metabolite analysis by GC-MS in six biological replicates. The heat maps show the log2 fold change between VOC treated plants and mock. Asterisks represent significant differences between bacterial treatments and mock (T-test, $p<0.05$, $n=6$). ND, not detected.